Energy Stress Regulates Hippo–YAP Signaling involving AMPK-mediated regulation of Angiomotin Like-1 Protein

Michael DeRan[1,5], Jiayi Yang[2,5], Che-Hung Shen[1,6], Eric C. Peters[2,6], Julien Fitamant[3], Puiyee Chan[1], Mindy Hsieh[2], Shunying Zhu[1], John M. Asara[4], Bin Zheng[1], Nabeel Bardeesy[3], Jun Liu[2] and Xu Wu[1,*]

[1] Cutaneous Biology Research Center, Massachusetts General Hospital, Harvard Medical School, Charlestown, Massachusetts, 02129

[2] Genomics Institute of the Novartis Research Foundation, San Diego, California, 92121

[3] Massachusetts General Hospital Cancer Center, Harvard Medical School, Boston, Massachusetts, 02114

[4] Division of Signal Transduction, Beth Israel Deaconess Medical Center, Harvard Medical School, Boston, Massachusetts, 02115

[5]These authors contributed equally

[6]These authors contributed equally

* Correspondence should be addressed to X.W.

Email: xwu@cbrc2.mgh.harvard.edu

Supplemental Information

1. Supplemental Results

Figure S1. High content imaging assay revealed energy stress inhibits YAP. Related to Figure 1.

A. Development of a high content imaging assay of YAP nuclear localization. HEK293A cells are cultures in sparse or dense conditions. Cells are fixed and stained with anti-YAP antibody and imaged under high content microscope. An algorithm measuring the correlation of YAP staining vs. nuclear staining is developed to quantify YAP nuclear localization. The Pearson's correlation between YAP positive area and nuclear staining was calculated to quantify YAP nuclear localization. R=1 (YAP in nuclei), R=-1 (YAP in cytoplasm); Density-dependent YAP localization validated the method and showed good dynamic window of the assay.
B. Metabolic stressors induce YAP cytoplasmic retention, and Comp C inhibits their effects. The images were associated with the graph in Figure 1a. Normalized YAP/nuclear Pearson's correlation is listed to quantify the level of YAP nuclear localization. Scale bar: 10μm.
C. HEK293A cells at low density culture were treated with DMSO control, AICAR (0.5 mM), or AICAR (0.5mM) and Compound C (10 μM) for 12h. Cells were subsequently fixed and immunostained for YAP (green) and the nuclei (Hoechst, blue). Scale bar: 5 μm.
D. A specific AMPK activator (A-768662) has similar effects on induction of p-YAP compared with energy stressor phenformin.
E. Glucose deprivation induces YAP Ser127 phosphorylation. Cells were cultured in normal medium (control, 4.5g/L glucose) or glucose free medium (Glucose –) for 12h. Cells were harvested for western blot analysis of p-YAP (Ser127) and total YAP. Protein levels were quantified by densitometry of the bands.
F. HEK293A cells were transfected with a YAP reporter plasmid (TEAD-binding element driven firefly luciferase) along with a p-CMV-Renilla-Luc plasmid. Cells at medium density (8000 cells/well) are cultured in normal media (no media change), glucose free media (Glucose –), adding back glucose (Glucose +) or serum free media (SFM, positive control). Firefly luciferase activities were read 14h after media change, and normalized to renilla luciferase controls (data are represented as mean, S.D. n=3, *, $p<0.01$, comparing to the Glucose + condition).
G. Energy stressors induce p-YAP (Ser127) in NIH3T3, OVCAR8 and HaCaT cells.
H-I. Anti-proliferative compounds such as inhibitors of PI3K, AKT, mTOR and CDK4 do not induce p-YAP. Cells were treated with DMSO control, Wortmannin (1μM), LY294002 (10 μM), rapamycin (100nM) for overnight, and p-YAP levels were analyzed by western blot (**H**). CDK inhibitor roscovitine was used at 10 μM to treat HEK293 cells at different time points (**I**).
I. Quantification of the colony sizes in YAP transformed MCF10A cells. The pixel area of each colony was measured by ImageJ.
J. Metformin (10mM) treatment inhibits YAP target genes expression (*CTGF* and *Cyr61*) in wild type YAP transduced MCF-10A cells. YAP (S127A) mutant transduced cells are largely resistant to metformin. Relative RNA levels were normalized to vector transduced MCF-10A cells (data are represented as mean, S.D. n=3).

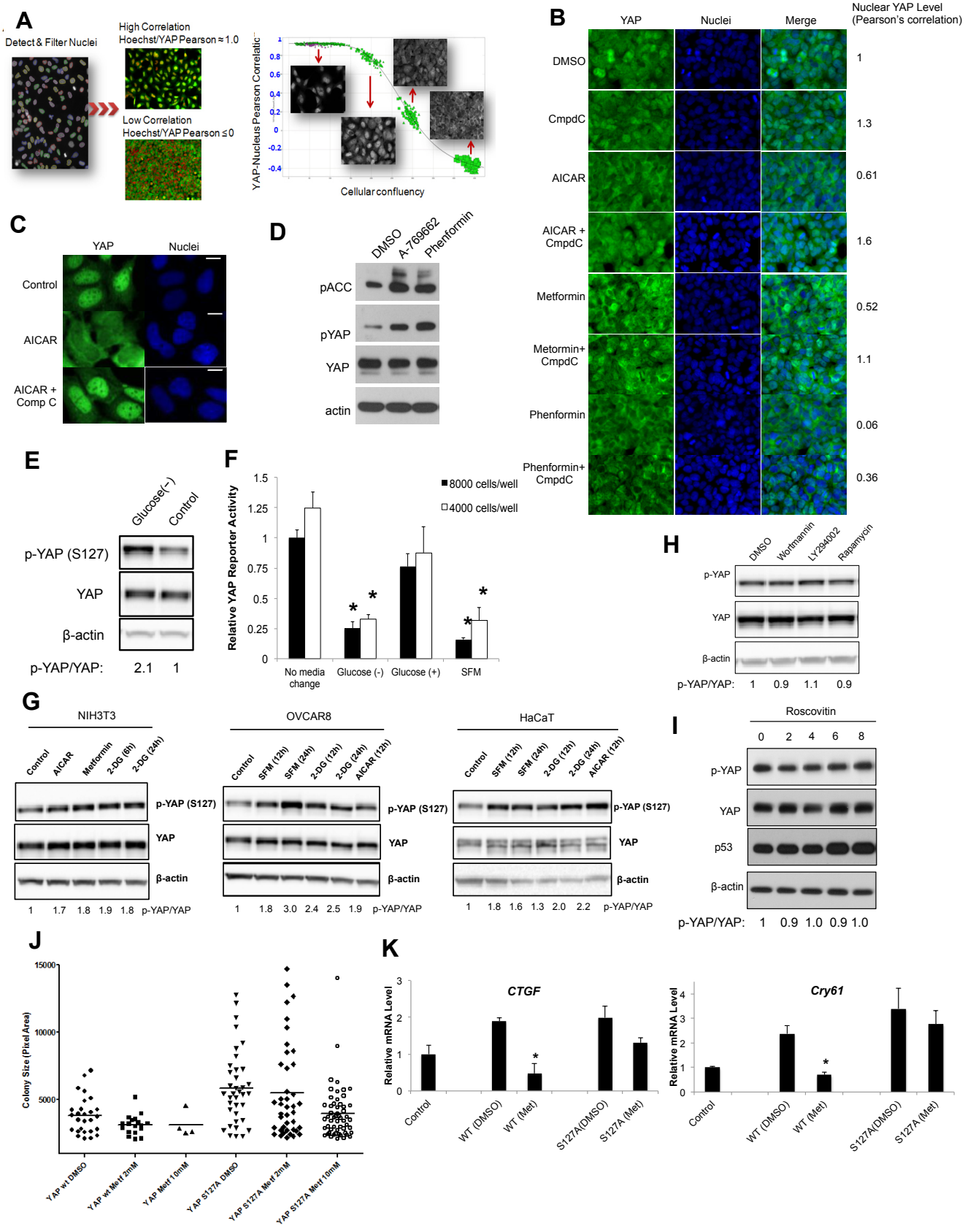
A
Detect & Filter Nuclei
High Correlation
Hoechst/YAP Pearson ≈ 1.0
Low Correlation
Hoechst/YAP Pearson ≤ 0
YAP-Nucleus Pearson Correlation
Cellular confluency
B
YAP
Nuclei
Merge
Nuclear YAP Level (Pearson's correlation)
DMSO
CmpdC
AICAR
AICAR + CmpdC
Metformin
Metormin+ CmpdC
Phenformin
Phenformin+ CmpdC
1
1.3
0.61
1.6
0.52
1.1
0.06
0.36
C
YAP
Nuclei
Control
AICAR
AICAR + Comp C
D
DMSO
A-769662
Phenformin
pACC
pYAP
YAP
actin
E
Glucose(-)
Control
p-YAP (S127)
YAP
β-actin
p-YAP/YAP: 2.1 1
F
Relative YAP Reporter Activity
8000 cells/well
4000 cells/well
No media change
Glucose (-)
Glucose (+)
SFM
H
DMSO
Wortmannin
LY294002
Rapamycin
p-YAP
YAP
β-actin
p-YAP/YAP: 1 0.9 1.1 0.9
G
NIH3T3
Control
AICAR
Metformin
2-DG (6h)
2-DG (24h)
p-YAP (S127)
YAP
β-actin
1 1.7 1.8 1.9 1.8 p-YAP/YAP
OVCAR8
Control
SFM (12h)
SFM (24h)
2-DG (12h)
2-DG (24h)
AICAR (12h)
p-YAP (S127)
YAP
β-actin
1 1.8 3.0 2.4 2.5 1.9 p-YAP/YAP
HaCaT
Control
SFM (12h)
SFM (24h)
2-DG (12h)
2-DG (24h)
AICAR (12h)
p-YAP (S127)
YAP
β-actin
1 1.8 1.6 1.3 2.0 2.2 p-YAP/YAP
I
Roscovitin
0 2 4 6 8
p-YAP
YAP
p53
β-actin
p-YAP/YAP: 1 0.9 1.0 0.9 1.0
J
Colony Size (Pixel Area)
YAP wt DMSO
YAP wt Met 2mM
YAP Met 10mM
YAP S127A DMSO
YAP S127A Met 2mM
YAP S127A Met 10mM
K
CTGF
Cry61
Relative mRNA Level
Control
WT (DMSO)
WT (Met)
S127A(DMSO)
S127A (Met)

Figure S2. AMPK and Lats1/2 are required to inhibit YAP. Related to Figure 2.
A. siRNA targeting AMPK α1α2 blocked YAP translocation induced by metformin and phenformin in HEK293A cells. Scale bar: 10 μm.
B. Knock-down efficiency of siRNAs targeting Lats1 and Lats2 as shown in Fig. 2e.

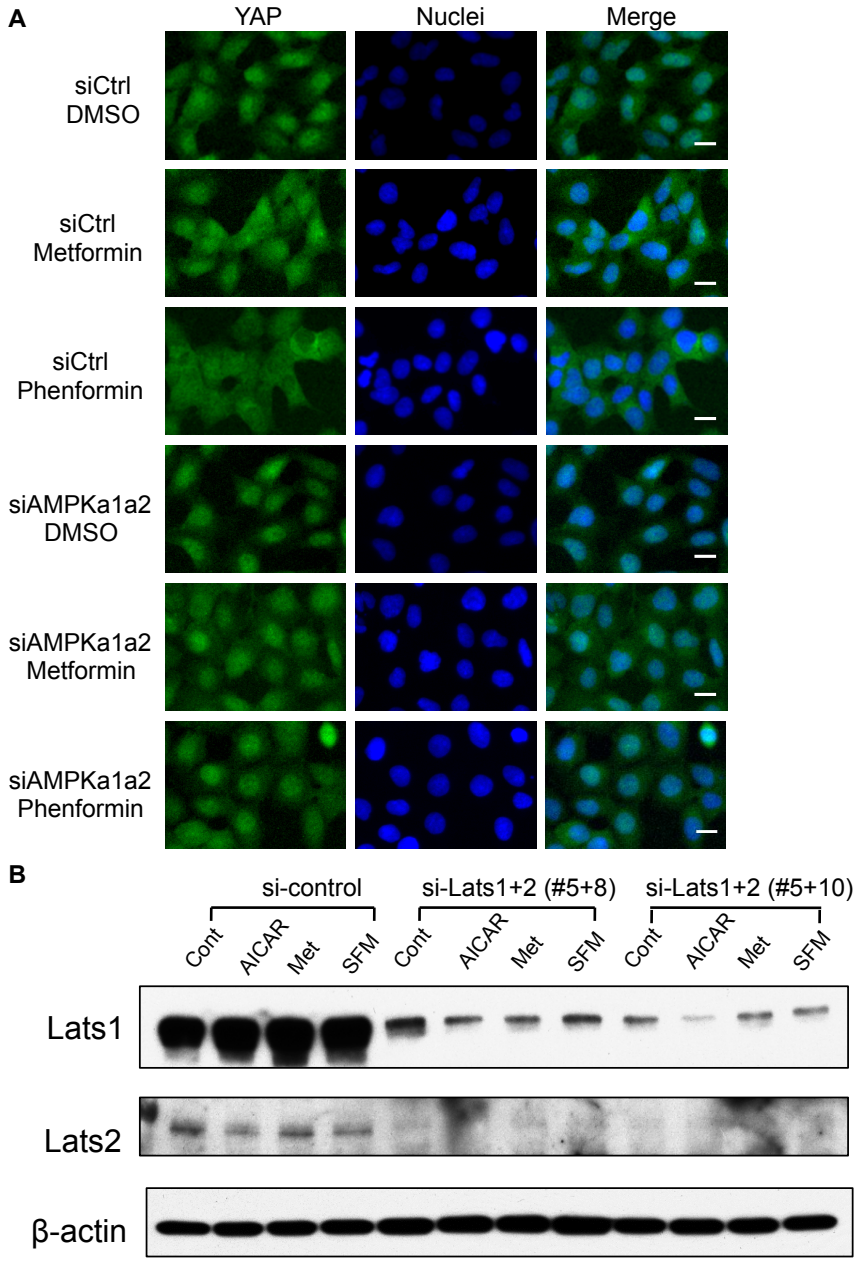

Figure S3. AMOTL1 is required to mediate the inhibition of YAP. Related to Figure 3.
A. qRT-PCR to detect the mRNA levels of AMOT, AMOTL1 and AMOTL2 upon metformin and phenformin treatment for 16h. (data are represented as mean, S.D. n=3)
B. Knock-down efficiency of siRNAs targeting AMOT and AMOTL1. Combination of siAMOT and siAMOTL1#3 showed good knock-down effeciecy for both genes, and was used in the experiments in **Figure. 3D**.
C. Representative images of YAP localization with AMOT and AMOTL1 silencing. The quantification was shown in Figure 4d. The white arrow shows the GFP positive transfected cells used in quantification. The GFP negative population was used as control. Scale bar: 10 μm.
D. shRNA knockdown of AMOTL1 rescues YAP target gene expression inhibition by phenformin.

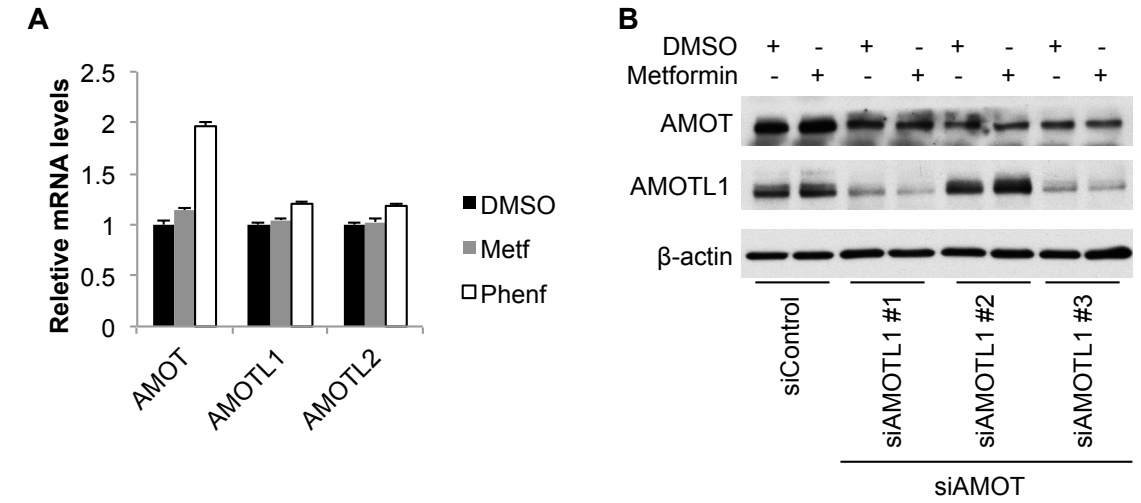
A
Reletive mRNA levels
2.5
2
1.5
1
0.5
0
AMOT
AMOTL1
AMOTL2
DMSO
Metf
Phenf
B
DMSO + - + - + - + -
Metformin - + - + - + - +
AMOT
AMOTL1
β-actin
siControl
siAMOTL1 #1
siAMOTL1 #2
siAMOTL1 #3
siAMOT

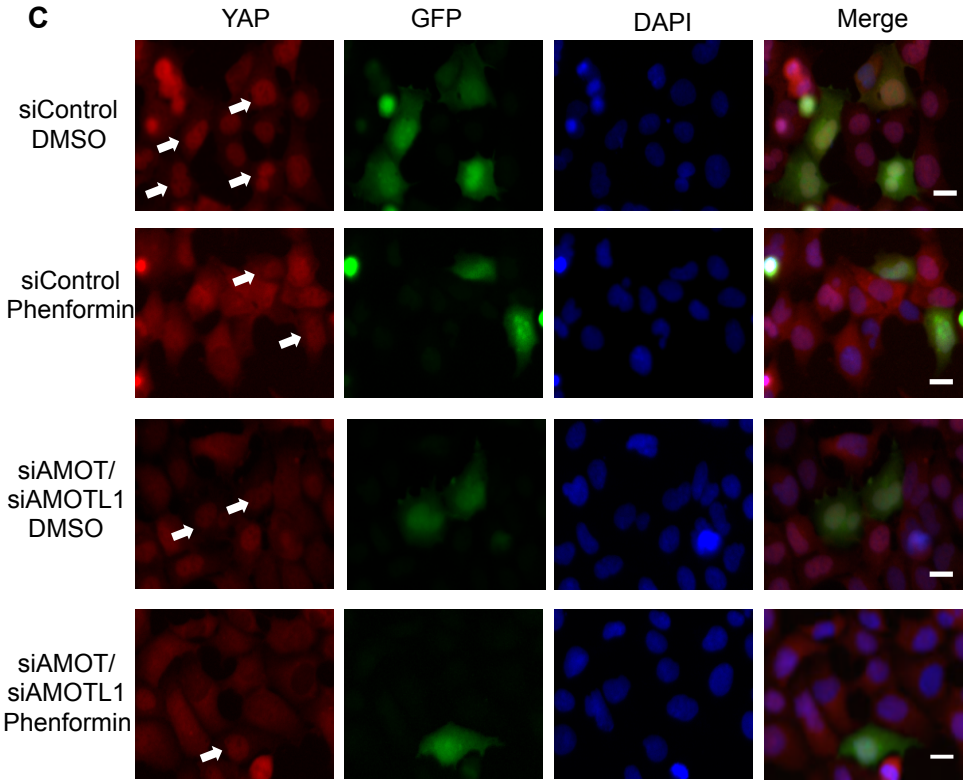
C
YAP
GFP
DAPI
Merge
siControl DMSO
siControl Phenformin
siAMOT/ siAMOTL1 DMSO
siAMOT/ siAMOTL1 Phenformin

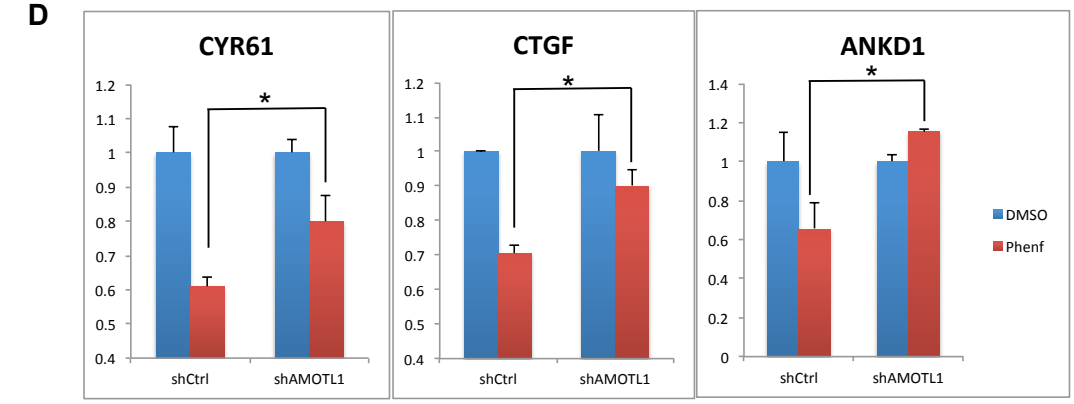
D
CYR61
CTGF
ANKD1
shCtrl
shAMOTL1
DMSO
Phenf

Figure S4. Phosphorylation studies of AMOT and AMOTL1. Related to Figure 4.

A. Flag-AMOTL1 co-immunoprecipitates with endogenous AMPKα.

B. Mass spectrometry studies of AMOTL1 phosphorylation. Tandem mass spectra of unphosphorylated and phosphorylated peptides confirm the site of the phosphorylation.

C. Phosphospecific antibody against p-AMOTL1 (Ser793) recognized wild type, but not AMOTL1 (Ser793Ala and Ser793Asp) mutants.

D. Compound C treatment decreases the half-life of endogenous AMOTL1 protein.

E. knockdown of Lats1/2 has little effects on AMPK activator (A-769662) induced AMOTL1 stablization.

F. HEK293A cells are infected with shRNA targeting AMOTL1, and then transfected with AMOTL1 wild type or S793A mutant. Cells were treated with DMSO control or phenformin for 24hours. YAP target gene expression is evaluated by qRT-PCR. Data are represented as mean, S.D. n=3. *, $p<0.05$ by comparing with the DMSO control.

G. Phosphoproteomic studies and in vitro kinase assays of AMOT

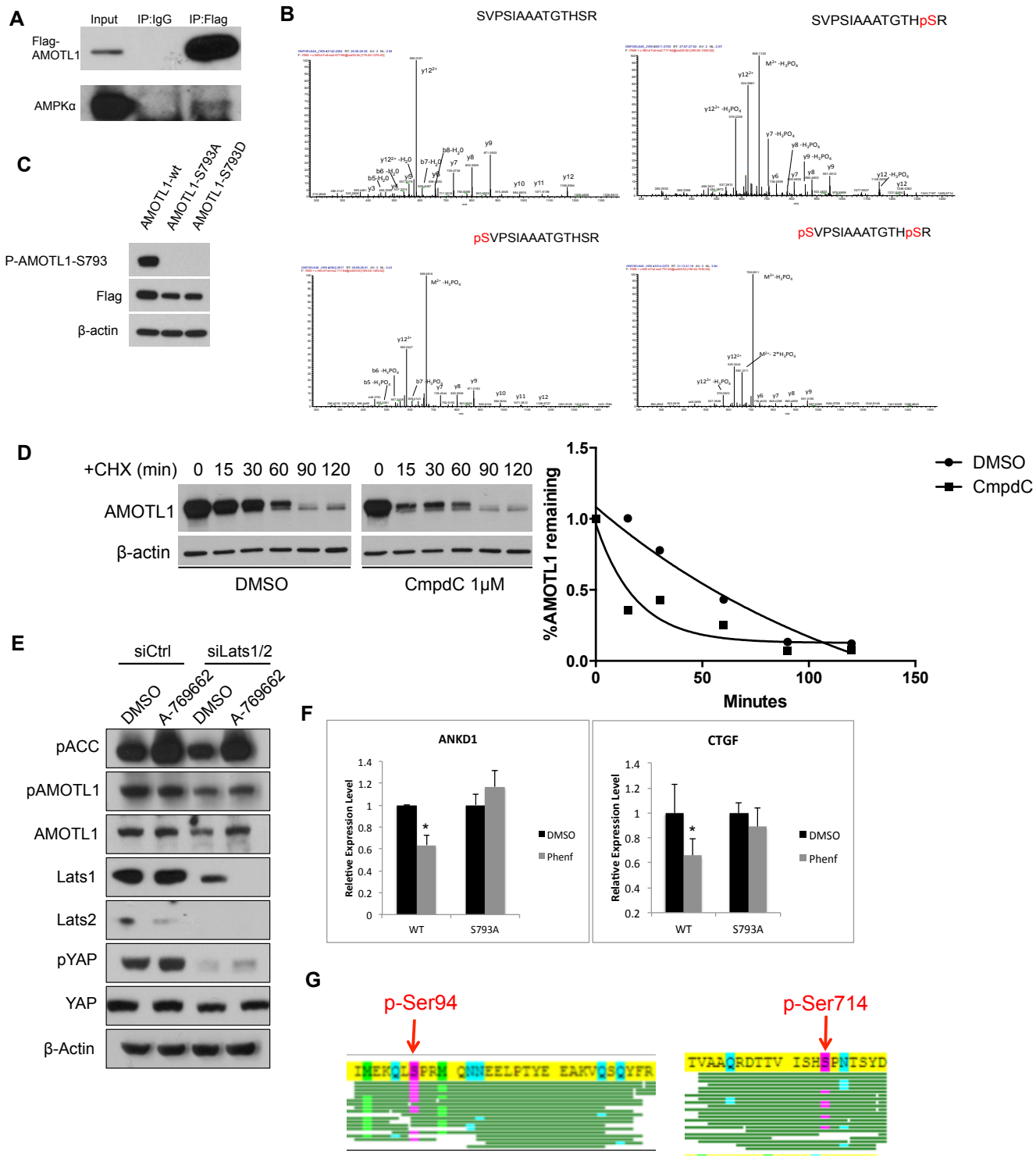
A
Input
IP:IgG
IP:Flag
Flag-AMOTL1
AMPKα
B
SVPSIAAATGTHSR
SVPSIAAATGTHpSR
pSVPSIAAATGTHSR
pSVPSIAAATGTHpSR
C
AMOTL1-wt
AMOTL1-S793A
AMOTL1-S793D
P-AMOTL1-S793
Flag
β-actin
D
+CHX (min) 0 15 30 60 90 120 0 15 30 60 90 120
AMOTL1
β-actin
DMSO
CmpdC 1μM
%AMOTL1 remaining
Minutes
DMSO
CmpdC
E
siCtrl
siLats1/2
DMSO
A-769662
DMSO
A-769662
pACC
pAMOTL1
AMOTL1
Lats1
Lats2
pYAP
YAP
β-Actin
F
ANKD1
CTGF
Reletive Expression Level
Relative Expression Level
DMSO
Phenf
WT
S793A
G
p-Ser94
p-Ser714

2. Supplemental Experimental Procedures

A. Cell culture

HEK-293A, NIH3T3, and HaCaT cell lines (purchased from ATCC, Manassas, VA) were maintained in Dulbecco's modified Eagles media (DMEM) supplemented with 10% fetal bovine serum (FBS) (Thermo/Hyclone, Waltham, MA). OVCAR8 cells were cultured in RPMI-1640 with 10% FBS. MCF10A cells were cultured in DMEM/F12 with 5% horse serum, 20 ng/mL EGF, 0.5 μg/mL hydrocortisone, 10 μg/mL insulin, 100 ng/mL cholera toxin and 50 μg/mL penicillin/streptomycin. For glucose deprivation, cells were plated in regular medium and allowed to attach overnight, then washed with PBS and changed into glucose (−) medium, which is glucose-deficient DMEM supplemented with 10% dialyzed FBS (Invitrogen) or glucose (+) medium, which is above medium plus 4.5 g/L D-glucose (Sigma), serving as a control.

B. Antibodies

Anti-YAP (M01) was purchased from Abgent (San Diego, CA) or Santa Cruz Biotechnology sc-101199) and used at a concentration of 0.2 μg/ml or 0.5ug/ml for immunofluorescent staining or western blot, respectively. Anti-p-YAP (Ser127) (#4911), anti-Lats1 (#3477), anti-Mst1 (#3682), anti-Mst2 (#3952), anti-AMPKα (#2532), anti-pAMPKα (#2535), p-14-3-3 motif (#9601), anti-pACC (#3661), anti-LKB1 antibodies were from Cell Signaling (Danvers, MA). Anti-β-actin (A-5441) was purchased from Sigma (St. Louis, MO), anti-Lats2 (ab70565) and anti-Mst2 (ab52641) were both purchased from Abcam (Cambridge, MA); anti-AMOT (sc-82491) and anti-NF2 (sc-332) were purchased form Santa Cruz Biotechnology and anti-AMOTL1 (HPA001196) antibody was purchased from Sigma-Aldrich; phosphospecific antibody anti-pAMOTL1 (Ser793) was generated by Abgent (San Diego, CA) by immunizing rabbits with peptides containing phosphorylated Ser793 of AMOTL1, and affinity purified

with the phosphopeptide. The specificity of the antibody is validated using phosphorylated peptide vs. non-phosphorylated peptide, and WT AMOTL1 vs. AMOTL1 (Ser793Ala and Ser793Asp) mutants. For immunofluorescent staining and Western Blot analyses, all antibodies were used according to manufacturers' recommended dilutions.

C. Chemicals

Compounds and their sources are: 2-deoxyglucose, phenformin, (Sigma-Aldrich); AICAR, metformin, Compound C, oligomycin, MG132, cycloheximide (Calbiochem). Compounds were prepared according to manufacturers' recommendations.

D. siRNA transfection

siRNA duplexes for human Lats1 (SI02223655, SI04438077), Lats2 (SI02660161, SI02660385), Mst1 (SI02622277, SI02637145), Mst2 (SI00086821, SI02622256), LKB1 (SI02665383, SI02777418, SI02777425), AMPK α1 (SI00086366, SI02622235), AMPK α2 (SI02758595, SI02758602), AMOT (SI04291385, SI04301283, AMOTL1 (SI04252115, SI04280815) and negative control (1027280) were obtained from Qiagen. siRNAs (final concentration= 25 nM) were reverse transfected into 293A cells in 6-well plates using Lipofectamine RNAiMAX (Invitrogen) or INTERFERin (Polyplus Transfection) according to the manufacturer's instructions. 48h post-transfection, cells were either harvested for silencing assessment or treated as indicated in the figures.

E. qRT-PCR experiment

YAP target gene expression was analyzed by TaqMan methods. Total RNAs were isolated and purified from cells cultured in 6-well dishes using PerfectPure RNA Cultured Cell Kit (5 Prime). Total RNAs

(200 ng) were then used for reverse transcription to synthesize the cDNAs using High Capacity cDNA Reverse Transcription Kit (Applied Biosystems). 5% of the resulting cDNA solution was used in the Taqman assay on 7900HT Fast Real-Time PCR System (Applied Biosystems), with probes detecting CTGF or CYR61, and GAPDH (Applied Biosystems).

Motin family member mRNA expression was analyzed with a LightCycler 480 (Roche). Total RNA was isolated from cells using TRIzol (Life Technologies) and then used to produce cDNA with the Transcriptor First Strand cDNA Synthesis Kit (Roche). The resulting cDNA was then used in reactions with the LightCycler 480 SYBR Green I Master mix (Roche). Primers used were AMOT F (ACCTCGTGAAGTCATCCTCCA), AMOT R (CCTCCGAATCTCGCCCTCTA), AMOTL1 F (GAAACATCTGCTTTGACGGTGG), AMOTL1 R (GAAGTTTGGGGAGTGGAAGTTAC), AMOTL2 F (ACCATGCGGAACAAGATGGAC), and AMOTL2 R (GAAGTTTGGGGAGTGGAAGTTAC).

F. Luciferase assay

HEK293A cells were seeded in 384-well format and transfected with the YAP reporter and a control Renilla luciferase construct using Fugene6 (Roche). The cells were then treated with various compounds. Luciferase assay was performed 24 h after treatment using the Dual Glo Luciferase System (Promega).

G. Western blot analysis

For AMPK phosphorylation experiments, cells are collected on ice and quickly frozen in liquid N_2 to reduce background phosphorylation. For other experiments, cells are collected on ice and directly lysed. Cell lysates were prepared by adding M-PER (Mammalian Protein Extraction Reagent, Fisher Scientific,

Pittsburg, PA), or RIPA buffer, supplemented with protease inhibitors (Roche Diagnostics) and phosphatase inhibitors (Sigma). Lysates were denatured by heating at 95 °C and loaded onto 4-12% Bis-Tris polyacrylamide gel, and subsequently transferred to nitrocellulose membrane (Bio-rad Laboratories, Hercules, CA) or polyvinylidene fluoride (Millipore). Membranes containing proteins were incubated with primary antibodies and secondary HRP-conjugated antibodies according to standard protocols, with chemiluminescent signal developed by adding SuperSignal Western substrates (Fisher Scientific) and captured by VersaDoc Imaging system (Bio-rad Laboratories), or developed by exposure to film.

H. Mass Spectrometry studies

Flag-tagged AMOTL1 was transfected in 293A cells. Cells were then treated with metformin, Compound C or DMSO control. Flag-AMOTL1 was immunoprecipitated. The proteins were digested by trypsin, and subjected to tandem mass spectrometry analysis. The mass spectrometer was set to acquire 1 full scan spectrum at 60,000 resolution in the orbitrap followed by CID of the top 20 ions in the linear ion trap. Dynamic exclusion was enabled allowing a repeat count of 3 with a duration of 15s and 60s exclusion time. The phosphor-peptides were then analyzed by MS/MS spectra. The abundance of the peptides was measured by AUC of the correspondent peaks on the ion chromatographs.

I. In vitro kinase assay

Flag-tagged AMOTL1 and their mutants were expressed in HEK293A cells and purified by immunoprecipitation. The proteins were then incubated with recombinant AMPK (Millipore) in kinase reaction buffer (25 mM MOPS pH 7.4, 25 mM $MgCl_2$, 12.5 mM b-glycerol-phosphate, 5 mM EGTA, 2 mM EDTA, 0.25 mM DTT, 100 μM AMP and 50 μM ATP) in the presence of γ-^{32}P-ATP (Perkin Elmer) at 37 °C for 30 min, followed by SDS-PAGE and autoradiography and liquid scintillation

counting. To evaluate the stoichiometry of phosphorylation, 1μg of substrate protein (350nM) and 50ng of enzyme (15nM) were used. The level of phosphate incorporation is quantified by liquid scintillation counting of the substrates using a standard curve of γ-^{32}P-ATP.

J. HCC cells from Mst1/2 liver knockout mice

Hepatocellular carcinoma cells were isolated from the Mst1/2$^{-/-}$ mice as described previously(Zhou et al., 2009). Mouse work was done with Institutional Animal Care and Use Committee approval at Massachusetts General Hospital Cancer Center, and in strict accord with good animal practice as defined by the Office of Laboratory Animal Welfare. The cells are cultured on rat tail collagen (BD Biosciences) in DMEM:Ham' F12 (1:1) medium supplemented with 10% heat inactivated fetal bovine serum, 1μg/mL insulin, 0.1μM dexamethasone, 10mM nicotinamide, 5mM HEPES, penicillin, and streptomycin. The cells were then transduced with YAP, YAP S127A, and stable clone were selected with puromycin.

K. MCF10A colony formation

YAP dependent MCF10A cell colony formation assay was performed as described previously(Debnath et al., 2003). Briefly, vector control, YAP or YAP S127A transduced cells were seeded in 8 well chamber slides. Cells were assayed in DMEM:F12 containing 2% horse serum, 0.5 μg/ml hydrocortisone, 100 ng/ml cholera toxin, 10 μg/ml insulin, penicillin, streptomycin, and the indicated compounds. The media was replaced every 4 days and the cells were imaged after 16-20 days of growth. Colony number was analyzed by counting the colonies from 4 random fields. Colony size was determined by measuring the area in pixels of the colonies using ImageJ.

3. Supplemental Discussion

We also observed that AMOTL1 Ser793 has a high basal phosphorylation level in HEK293A cells, and inhibition of basal AMPK activities by Compound C treatment or siRNA-mediated silencing of AMPKα1α2 quickly decreases its protein level, suggesting that basal AMOTL1 Ser793 phosphorylation may maintain its stability and contribute to tight junction assembly. It is known that AMPK could be activated through Ca^{2+} /calmodulin-dependent protein kinase kinase β (CaMKKβ) independent of energy stress, and calcium played an important role in maintaining cellular tight junctions (Denker and Nigam, 1998; Hardie, 2007; Hawley et al., 2005; Woods et al., 2005). It is possible that CaMKKβ-mediated AMPK activation accounts for the high background of AMOTL1 phosphorylation and its basal stability. Indeed, it has been reported previously that calcium promotes tight junction assembly through AMPK (Zhang et al., 2006; Zheng and Cantley, 2007), although the detailed mechanisms are still unclear. Our results might provide some mechanistic insights to these processes and suggest that AMPK-mediated direct phosphorylation of AMOTL1 might lead to the stabilization of TJ.

Recently, *Drosophila* salt-inducible kinases (SIK1 and 2), members of the AMPK family of kinases, have been implicated as activators of Yorkie. Different from the effects of mammalian AMPK we described in this paper, fly SIK kinases increase Yki target expression and promote tissue overgrowth through phosphorylation of Sav(Wehr et al., 2013). However, there are no homologues of AMOT family protein in *Drosophila*, and we did not identify an AMPK substrate motif in SAV1. Therefore, AMPK-mediated AMOTL1 regulation could be specific to mammals, suggesting a divergent regulation of this pathway in fly and mammals(Bossuyt et al., 2013). Whether SIK could phosphorylate AMOTL1 S793 requires further investigation. It was also discovered recently that YAP could regulate the systemic

nutrient sensing PI3K/PTEN/mTOR pathway through miRNA-mediated mechanisms, suggesting that Hippo pathway and cellular metabolic pathways indeed form a highly orchestrated network at multiple levels(Tumaneng et al., 2012).

A recent study has demonstrated that LKB1 is an upstream regulator of YAP activity. Interestingly, the authors showed that LKB1 acts through the microtubule affinity-regulating kinase (MARK) family to regulate the localization of Scribble(Mohseni et al., 2014). While the authors did not observe that suppression of either AMPK α1 or α2 could rescue the effects of LKB1 activation on YAP, they did not investigate whether suppression of both AMPK α1 and α2 could rescue this effect. Thus compensatory effects could explain why the authors did not find AMPK to mediate the LKB1-induced YAP inactivation. However, taken together our results and the results of Mohseni et al suggest that there are multiple pathways downstream of LKB1 regulating YAP activity.

In clinical and preclinical studies, AMPK activators (metformin, phenformin and AICAR) have shown encouraging anti-tumor activities(Shackelford and Shaw, 2009). Inhibition of YAP might be part of the mechanisms mediating their anti-tumor effects. In the treatment of type II diabetes, metformin mediates the effects at micromolar concentrations in vivo. This is largely due to the expression of organic cation transporters (OCTs) in liver cells, which actively transport metformin into liver cells, the primary site of action to lower glucose levels(Shu et al., 2007). Many other cell types (including HEK293A, and many cancer cell lines) do not express OCTs; therefore, higher doses of metformin are needed to activate AMPK. It is possible that phenformin which does not require OCTs to enter the cells, might be a more potent and suitable compound to treat many YAP-dependent cancers lacking OCTs. Further in vivo

preclinical and clinical studies are needed to evaluate whether pharmacological activation of AMPK could be therapeutically useful for YAP-dependent cancers.

4. Supplemental References

Adler, J.J., Johnson, D.E., Heller, B.L., Bringman, L.R., Ranahan, W.P., Conwell, M.D., Sun, Y., Hudmon, A., and Wells, C.D. (2013). Serum deprivation inhibits the transcriptional co-activator YAP and cell growth via phosphorylation of the 130-kDa isoform of Angiomotin by the LATS1/2 protein kinases. Proc Natl Acad Sci U S A *110*, 17368-17373.

Bossuyt, W., Chen, C.L., Chen, Q., Sudol, M., McNeill, H., Pan, D., Kopp, A., and Halder, G. (2013). An evolutionary shift in the regulation of the Hippo pathway between mice and flies. Oncogene.

Dai, X., She, P., Chi, F., Feng, Y., Liu, H., Jin, D., Zhao, Y., Guo, X., Jiang, D., Guan, K.L*., et al.* (2013). Phosphorylation of angiomotin by Lats1/2 kinases inhibits F-actin binding, cell migration and angiogenesis. J Biol Chem.

Debnath, J., Muthuswamy, S.K., and Brugge, J.S. (2003). Morphogenesis and oncogenesis of MCF-10A mammary epithelial acini grown in three-dimensional basement membrane cultures. Methods *30*, 256-268.

Denker, B.M., and Nigam, S.K. (1998). Molecular structure and assembly of the tight junction. Am J Physiol *274*, F1-9.

Hardie, D.G. (2007). AMP-activated/SNF1 protein kinases: conserved guardians of cellular energy. Nat Rev Mol Cell Biol *8*, 774-785.

Hawley, S.A., Pan, D.A., Mustard, K.J., Ross, L., Bain, J., Edelman, A.M., Frenguelli, B.G., and Hardie, D.G. (2005). Calmodulin-dependent protein kinase kinase-beta is an alternative upstream kinase for AMP-activated protein kinase. Cell Metab *2*, 9-19.

Mohseni, M., Sun, J., Lau, A., Curtis, S., Goldsmith, J., Fox, V.L., Wei, C., Frazier, M., Samson, O., Wong, K.K*., et al.* (2014). A genetic screen identifies an LKB1-MARK signalling axis controlling the Hippo-YAP pathway. Nat Cell Biol *16*, 108-117.

Nguyen, H.B., Babcock, J.T., Wells, C.D., and Quilliam, L.A. (2012). LKB1 tumor suppressor regulates AMP kinase/mTOR-independent cell growth and proliferation via the phosphorylation of Yap. Oncogene *Published online Oct. 3rd*, 10.1038/onc.2012.1431.

Shackelford, D.B., and Shaw, R.J. (2009). The LKB1-AMPK pathway: metabolism and growth control in tumour suppression. Nature reviews. Cancer *9*, 563-575.

Shu, Y., Sheardown, S.A., Brown, C., Owen, R.P., Zhang, S., Castro, R.A., Ianculescu, A.G., Yue, L., Lo, J.C., Burchard, E.G*., et al.* (2007). Effect of genetic variation in the organic cation transporter 1 (OCT1) on metformin action. J Clin Invest *117*, 1422-1431.

Tumaneng, K., Schlegelmilch, K., Russell, R.C., Yimlamai, D., Basnet, H., Mahadevan, N., Fitamant, J., Bardeesy, N., Camargo, F.D., and Guan, K.L. (2012). YAP mediates crosstalk between the Hippo and PI(3)K-TOR pathways by suppressing PTEN via miR-29. Nat Cell Biol *14*, 1322-1329.

Wehr, M.C., Holder, M.V., Gailite, I., Saunders, R.E., Maile, T.M., Ciirdaeva, E., Instrell, R., Jiang, M., Howell, M., Rossner, M.J*., et al.* (2013). Salt-inducible kinases regulate growth through the Hippo signalling pathway in Drosophila. Nat Cell Biol *15*, 61-71.

Woods, A., Dickerson, K., Heath, R., Hong, S.P., Momcilovic, M., Johnstone, S.R., Carlson, M., and Carling, D. (2005). Ca2+/calmodulin-dependent protein kinase kinase-beta acts upstream of AMP-activated protein kinase in mammalian cells. Cell Metab *2*, 21-33.

Yi, C., Shen, Z., Stemmer-Rachamimov, A., Dawany, N., Troutman, S., Showe, L.C., Liu, Q., Shimono, A., Sudol, M., Holmgren, L*., et al.* (2013). The p130 isoform of angiomotin is required for Yap-mediated hepatic epithelial cell proliferation and tumorigenesis. Sci Signal *6*, ra77.

Zhang, L., Li, J., Young, L.H., and Caplan, M.J. (2006). AMP-activated protein kinase regulates the assembly of epithelial tight junctions. Proc Natl Acad Sci U S A *103*, 17272-17277.

Zheng, B., and Cantley, L.C. (2007). Regulation of epithelial tight junction assembly and disassembly by AMP-activated protein kinase. Proc Natl Acad Sci U S A *104*, 819-822.

Zhou, D., Conrad, C., Xia, F., Park, J.S., Payer, B., Yin, Y., Lauwers, G.Y., Thasler, W., Lee, J.T., Avruch, J*., et al.* (2009). Mst1 and Mst2 maintain hepatocyte quiescence and suppress hepatocellular carcinoma development through inactivation of the Yap1 oncogene. Cancer Cell *16*, 425-438.